

Orbital remote sensing to estimate evapotranspiration in a cotton cropping system irrigated by a centre pivot

Wendel Kaian Mendonça Oliveira^{1*}, Marcio Furlan Maggi¹, Luan Peroni Venancio², Claudio Leones Bazzi³, Lúcia Helena Pereira Nóbrega¹, Erivelto Mercante¹

¹Universidade Estadual do Oeste do Paraná, Programa de Pós-Graduação em Engenharia Agrícola, Rua Universitária, 2069, JD. Universitário - Prédio de Desenvolvimento de Protótipos, CEP 85819-110, Cascavel, Paraná, Brazil

²Universidade Federal de Viçosa, Departamento de Engenharia Agrícola, Programa de Pós-Graduação em Engenharia Agrícola, CEP 36570-900, Viçosa, Minas Gerais, Brazil

³Universidade Tecnológica Federal do Paraná, Departamento de Ciência da Computação, Avenida Brasil, 4232, CEP 85884-000, Medianeira, Paraná, Brazil

*Corresponding author: wendel.moreira@unioeste.br

Abstract

Evapotranspiration (ET) estimation is essential for adequate management of water resources. The main ways to quantify ET are based on the use of field sensors, class A tanks, Bowen's ratio method, turbulent vortex correlation analysis, use of lysimeters, and through Remote Sensing (RS), which allows estimating biophysical parameters based on satellite images. The objective of the research was to determine the effective evapotranspiration (ET_e) of cotton plantations irrigated with a centre pivot, using the Surface Energy Balance Algorithm for Land (SEBAL), Mapping Evapotranspiration at High Resolution and with Internalized Calibration (METRIC) and Simple Algorithm for Evapotranspiration Retrieving (SAFER) methods. Comparisons were made for three agricultural years, using the R^2 , RMSE, MAE, MBE and R statistics. The best performances in the crops were obtained with the SEBAL vs. SAFER models, which presented mean values of 0.54, -0.30 and 0.31 $mm\ d^{-1}$ in RMSE, MBE and MAE, respectively. The data obtained by all three models can be applied to estimate ET_e in irrigated cotton plantations and, consequently, their results can assist in irrigation management and in crop treatments.

Keywords: irrigation, water demand, transpiration, energy balance.

Abbreviations: SEBAL_Surface Energy Balance Algorithm for Land; METRIC_Mapping Evapotranspiration at High Resolution and with Internalized Calibration; SAFER_Simple Algorithm for Evapotranspiration Retrieving; TSM_Two-Source Models our Two-Layer Models; TMEF_A Two-Source Model for Estimating Evaporative Fraction; WSITSEBM_Wind Speed-Independent Two-Source Energy Balance Model; LE_Latent Heat Flux.

Introduction

It is estimated that 70% of water use in agriculture is for irrigation (FAO, 2021) and sustainable use of this resource has become a global concern, considering, in addition to the increased demand, the reduction in the water available due to climatic, vegetation and soil factors. In this context, numerous studies have been carried out with the objective of obtaining accurate evapotranspiration (ET) data, considering that they allow detecting water stress in crops, which is essential to optimize irrigation systems so that they use less water (Pradipta et al., 2022) and to evaluate the hydrological cycle dynamics.

ET corresponds to the sum of water loss by the plant (transpiration) and by the surface (evaporation) and can be defined in four ways: 1) reference evapotranspiration (ET_0); 2) effective evapotranspiration (ET_e); 3) oasis evapotranspiration (ET_o); and 4) crop evapotranspiration (ET_c). This latter depends on the crop coefficient (K_c), which varies predominantly according to the specific characteristics of each crop, phenological state and soil

moisture (Allen et al., 1998). ET can be quantified by: 1) data obtained through stations; 2) making use of pan evaporation; 3) using the Bowen ratio method; 4) turbulent vortex correlation analysis; 5) using lysimeters; and 6) using Remote Sensing (RS) data based on the Earth's surface temperature (LTS or T_s) (Mkhwanazi et al., 2015; Jensen and Allen, 2016).

Due to practical application and reduced cost, by using RS it is possible to perform ET estimates from energy balance models, in which evaporation is calculated as a residual (Jensen and Allen, 2016). The models to estimate ET can be classified according to the number of sources (Single Source Models - SSMs and Two-Source Models - TSMs).

SSMs generally use the Earth's surface temperature as a proxy for aerodynamic temperature (T_{ao}) to calculate sensible heat flux (H). Examples of these types of widely used models include *Surface Energy Balance Algorithm for Land* (SEBAL) (Bastiaanssen et al., 1998), *Mapping Evapotranspiration at High Resolution and with Internalized*

Calibration (METRIC) (Allen et al., 2007) and *Simple Algorithm for Evapotranspiration Retrieving* (SAFER) (Teixeira and Hernandez, 2012).

TSMs calculate estimates of sensible and latent heat fluxes from the soil and canopy components of vegetated surfaces. The components of the latent heat flux can be converted into evaporation (E), transpiration (T) and, when combined, into evapotranspiration (ET) (Colaizzi et al., 2014; Sun, 2016). Examples of these types of models include the Two-Source Models our Two-Layer Models (TSMs) (Norman et al., 1995), Two-Source Model for Estimating Evaporative Fraction (TMEF) (Sun, 2016) and Wind Speed-Independent Two-Source Energy Balance Model (WSITSEBM) (Wang et al., 2020). The disadvantage of TSMs is linked to their complexity; however, what has been a real impediment to their more widespread use is the scarcity of E or T measurements, which limits most of the TSEB model studies to only considering latent heat flux (LE) or ET (Colaizzi et al., 2002).

Despite this, SSMS have provided satisfactory energy flux estimates for heterogeneous surfaces, in addition to being applied in various weather and vegetation conditions (Barker et al., 2018; Yang et al., 2022) and for requiring few surface meteorological data, which makes them useful for places where these data are limited (Mkhwanazi et al. 2015). Among the SSMS that have been used for application in agricultural areas, SEBAL can be highlighted, which has been tested in more than 30 countries with acceptable precision varying from 85% to 95% in daily and seasonal scales (Bastiaanssen et al., 2000).

Considering the diversity of RS models for ET estimation, studies seeking to compare them are essential to determine which are more efficient in determining crop, soil and weather conditions. Thus, this research aims at determining the effective evapotranspiration (ET_e) of cotton plantations irrigated by a centre pivot system, using three different models: SEBAL, METRIC and SAFER, where, due to the reliability obtained from the literature, the SEBAL model was considered as the standard.

Results and discussion

Meteorological conditions

Figure S1 presents the monthly mean values of temperature (T_m), extraterrestrial solar radiation (Ra), wind speed (WS), relative humidity (RH) in the air, reference evapotranspiration (ET_0) and rainfall. The T_m and RH of the air remained close over all three years, with variations in T_m lower than 1°C across the years. In the case of RH, the variations were lower than 1%. With regard to the mean values, 23.58°C and 68.9% were verified for T_m and RH, respectively, which are very close to the historical mean of the region. T_m presented a mean of 24.5°C in the two initial months, for the three years, period in which cotton was planted in the field and, according to Walne et al. (2020), this is close to the values recommended for successful germination.

WS presented a variation considered large between 2018 and 2020 with mean values of 0.32 and 1.1 $m s^{-1}$, respectively (Figure S1C). The cotton crop lasted a mean of 181 days and, in the study area, the sowing window normally starts in the first half of June and ends in early July. It is important to highlight that rainfall is higher between February and March, with a reduction in its volume since May (Figure S1F), extending until the end of September.

Entry parameters of the models

The comparison between all three surface energy balance models (SEBAL, METRIC and SAFER) is presented below. The input parameters (Digital Elevation Model [DEM], Surface albedo [Sa], Normalized Difference Vegetation Index [NDVI] and Surface temperature [T_s]) are described:

The altitude that was generated based on DEM is an important variable to assess and identify variability in the relief, which in turn influences T_s ; therefore, the METRIC and SEBAL algorithms use this parameter to adjust that variable. The regions between pivots P5 and P12 present the highest altitudes according to the spatial map and to the boxplot, and pivot P8 had the highest altitude when compared to the others (Figure S2).

The ratio between incident and reflected short-wave radiation is called reflection coefficient or Sa, which can be thought of as the Earth's reflectivity, that is, the amount of incoming sunlight that is reflected back into space (Acker et al., 2014). Considered as a first-order determinant of energy flow, which can be influenced by factors such as humidity and temperature (Small, 2006), it is employed in the SEB models providing surface reflectance information for the calculation of net radiation.

Sa presented a mean value of 0.15 for all methods and years studied, and SAFER had a lower value when compared to METRIC and SEBAL (Figure S3). Time distribution of Sa is increasing, closely following development of the crop, and the highest values can be observed since April for all methods; however, it was not possible to notice large variations between the pivots in the spatial comparison. P4 presented the highest Sa across all three methods and agricultural years (2018, 2019 and 2020), together with P7, P8, P9 and P10 (Figure S3).

Where this vegetation index is used to describe the general effect of vegetation on the surface flows and, therefore, its application is in estimating soil heat flux (G) and roughness length (Z_{om}) in the SEBAL and METRIC models (Bastiaanssen et al., 1998; Allen et al., 2007). NDVI is a key RS indicator related to land cover and soil moisture, and the long-wave radiation emitted is directly proportional to T_0 (Teixeira et al., 2012).

NDVI has a peculiar characteristic for all the images evaluated: a low value > 0.37 corresponding to the months of January, February and the end of June (it corresponds to physiological stage I and beginning of stage II, and end of stage IV) and with expressive growth with progress of cotton's physiological development, reaching its highest value (0.89) (it corresponds to physiological stage III) (Figure S4). The NDVI equation is standard; thus, the NDVI images generated by the SEBAL algorithm were applied in SAFER; therefore, the NDVI maps are identical to each other. T_s is a source of conductive, convective and radiant energy transfer, as well as a direct measure of the thermal environment on the surface (Pianalto and Yool, 2017). Using RS, the T_s values are calculated from satellite image information regarding thermal radiance (Sánchez-Aparicio et al., 2020), they can be applied to investigate time and spatial changes in land use/cover (Jensen, 2000), and their relationship with reflectance can provide information about the surface properties (for example: composition, emissivity) and also about the processes (for example: evapotranspiration, latent and sensible heat flux), which are the main determinants of surface energy balance (Small, 2006; Allen et al., 2011).

Table 1. Sowing date (SD), harvest date (HD), cycle length in days (Cycle) and variety (Va) for 2018, 2019 and 2020, with cotton plantations.

Pivot	2018				2019				2020			
	Va	SD	HD	Cycle	Va	SD	HD	Cycle	Va	SD	HD	Cycle
P1	-	-	-	-	FM 975	Jan/09	Jul/10	182	-	-	-	-
P2	-	-	-	-	-	-	-	-	-	-	-	-
P3	FM 983	Jan/02	May/08	185	-	-	-	-	-	-	-	-
P4	-	-	-	-	FM 975	Jan/09	Jul/10	182	-	-	-	-
P5	FM 975	Jan/02	May/08	185	-	-	-	-	FM 975	Jan/01	May/07	177
P6	-	-	-	-	-	-	-	-	-	-	-	-
P7	FM 975	Jan/02	May/08	185	-	-	-	-	-	-	-	-
P8	-	Jan/05	May/04	180	-	-	-	-	-	-	-	-
P9	-	-	-	-	-	-	-	-	FM 975	Jan/01	May/07	177
P10	-	-	-	-	-	-	-	-	-	-	-	-
P11	-	-	-	-	-	-	-	-	-	-	-	-
P12	TMG 47	Jan/02	May/08	185	-	-	-	-	-	-	-	-

- Cotton was not planted.

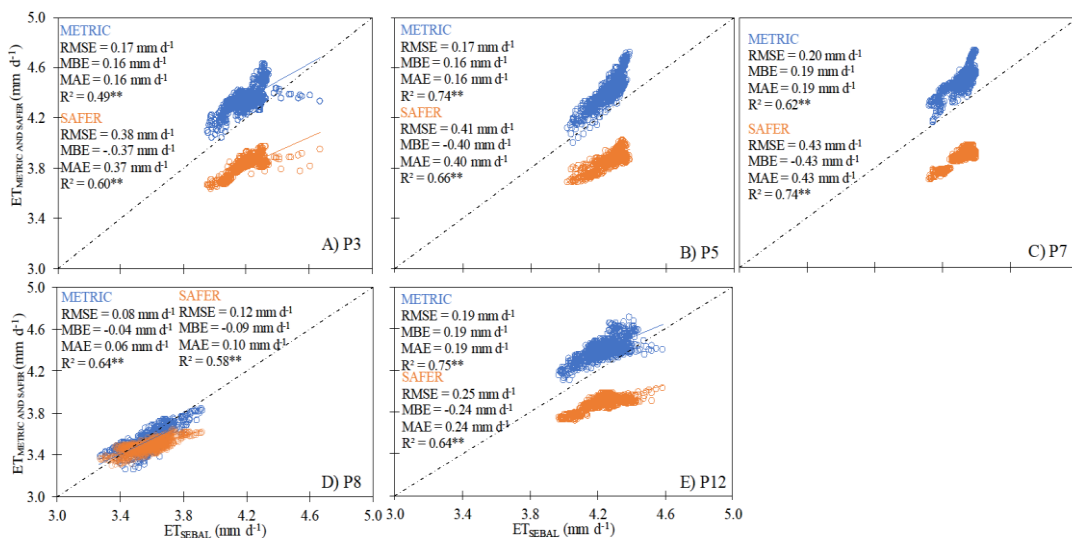


Fig 1. Effective evapotranspiration comparisons: ET_{SEBAL} (mm d⁻¹) vs ET_{METRIC} (mm d⁻¹) and ET_{SEBAL} (mm d⁻¹) vs ET_{SAFER} (mm d⁻¹), for 2018. The dotted black lines represent the 1:1 line and the coloured dotted lines represent the linear regressions. P: Centre Pivot. **Significance of the regression at p-value<0.001.

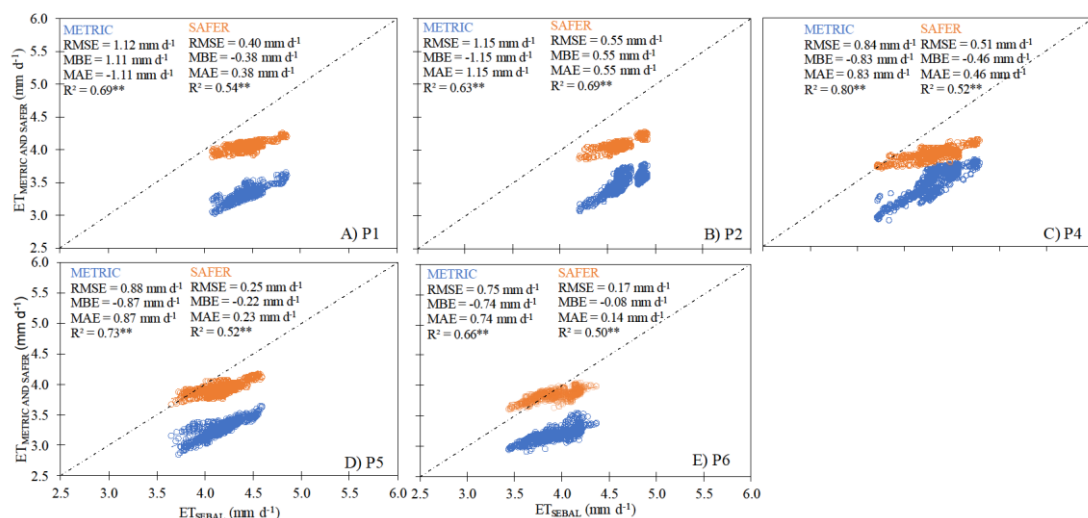


Fig 2. Effective evapotranspiration comparisons: ET_{SEBAL} (mm d⁻¹) vs ET_{METRIC} (mm d⁻¹) and ET_{SEBAL} (mm d⁻¹) vs ET_{SAFER} (mm d⁻¹), for 2019. The dotted black lines represent the 1:1 line and the coloured dotted lines represent the linear regressions. P: Centre Pivot. **Significance of the regression at p-value<0.001.

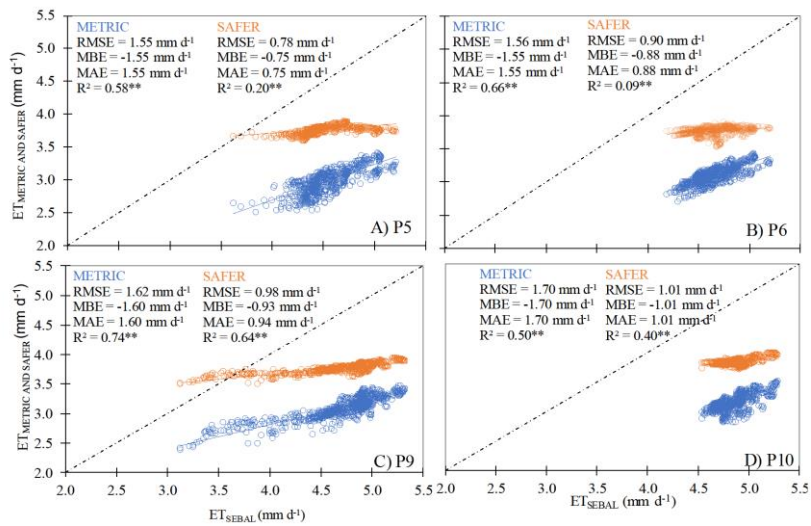


Fig 3. Effective evapotranspiration comparisons: ET_{SEBAL} ($mm\ d^{-1}$) vs ET_{METRIC} ($mm\ d^{-1}$) and ET_{SEBAL} ($mm\ d^{-1}$) vs ET_{SAFER} ($mm\ d^{-1}$), for 2020. The dotted black lines represent the 1:1 line and the coloured dotted lines represent the linear regressions. P: Centre Pivot. **Significance of the regression at p -value<0.001.

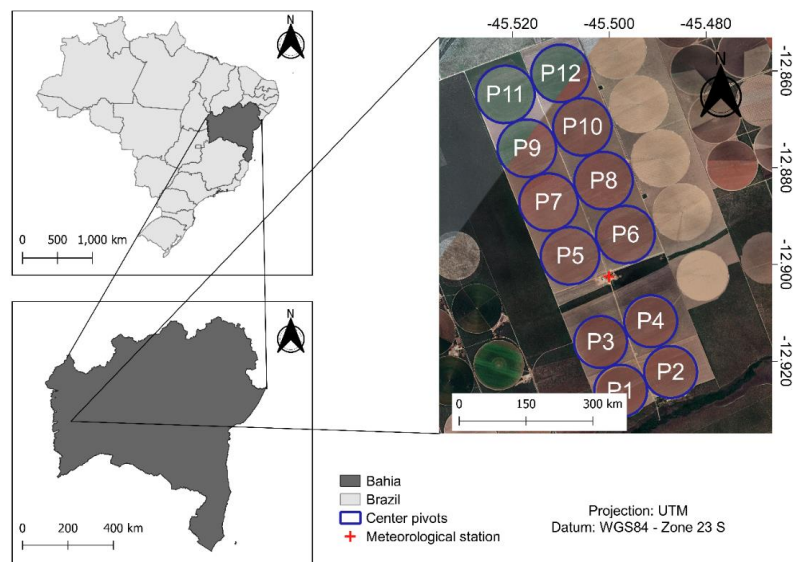


Fig 4. Commercial farm location map.

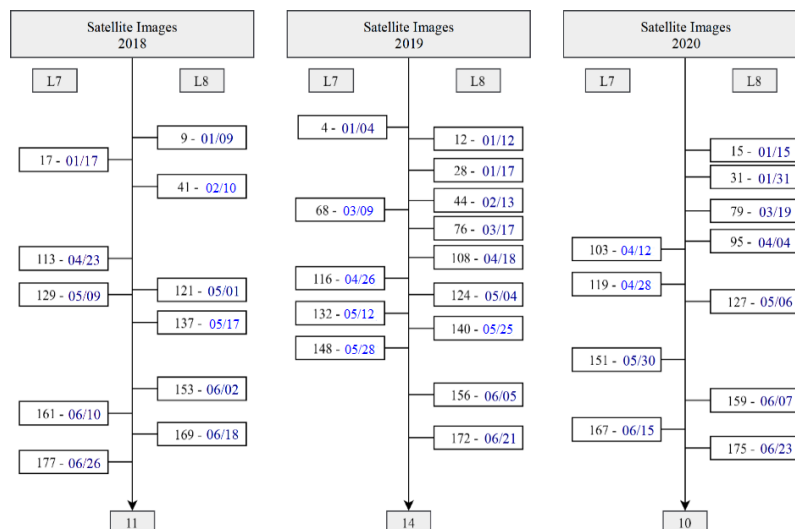


Fig 5. Images selected for evapotranspiration estimation: in blue, the date corresponding to each image; and in black, the Julian Day.

In this context, T_s is an important tool as input data for ET calculation, as it describes the surface condition and the partition of available energy in H and LE (Kustas and Norman, 1996). Therefore, the spatial and time distribution of T_s for all three methods (SEBAL, METRIC and SAFER) and agricultural years (2018, 2019 and 2020) can be seen in Figure S8. The highest T_s values are normally observed at the beginning and at the end of cotton cropping, when there is bare soil or low incidence of vegetation cover, due to the crop's senescence stage. In addition to that, it is possible to notice that, in 2019, T_s was relatively higher than in the other periods studied (Figure S5).

SAFER presented the lowest T_s values when compared to the METRIC and SEBAL methods; this is because, due to being an empirical equation, its calibration was adjusted for the semiarid region. Another important condition is that T_s affects the available energy, acting on the long-wave radiation balance, with lower values under irrigation conditions than in the drier areas around the irrigated plots (Teixeira et al., 2017).

The lowest T_s values were observed in 2018, with the highest values recorded in the initial stages, which corresponds to the month of January and with a reduction between the period from April to early June (Figure S5). This low variation is a consequence of total soil coverage by the crop, of the low variation in the weather conditions over the three years, and of the low variation in the cropping system and irrigation management (Venancio et al., 2020).

The SEBAL model presented the highest ET in 2020, with a mean value of 4.24 mm d^{-1} across the pivots, with pivot P09 reaching 5.32 mm d^{-1} .

Figures 1, 2 and 3 present the comparisons made between the ET estimation methods ($ET_{SEBAL} [\text{mm d}^{-1}]$ vs $ET_{METRIC} [\text{mm d}^{-1}]$ and $ET_{SEBAL} [\text{mm d}^{-1}]$ vs $ET_{SAFER} [\text{mm d}^{-1}]$) for all three agricultural years; and, for validation of the models, coefficient of determination (R^2), Root Mean Square Error (RMSE), Mean Bias Error (MBE) and Mean Absolute Error (MAE) were used between the comparisons performed.

The scatter plots show that there is certain degree of linearity between the comparisons, and the SEBAL vs METRIC comparison presented the best data dispersions. According to Singh and Senay (2016), who studied different methods for estimating ET_c , good linearity was found across the methods, and it was indicated that all models captured the spatial variability of the instantaneous ET and of the evaporative fraction.

The R^2 coefficient varied from 0.1 to 0.8 with a mean of 0.6 across all centre pivots and for all three years, and the SEBAL vs METRIC comparisons presented the highest agreement in their results, whereas the comparisons made between SEBAL and SAFER for the three agricultural years presented mean values of 0.54, -0.30 and 0.31 mm d^{-1} in RMSE, MBE and MAE respectively (Figures 1, 2 and 3). The studies by Filgueiras et al. (2019) noticed that the mean difference between the ET_a -SEBAL and ET_a -EEFLUX products was 0.20 mm.

The highest ET values were observed in the SEBAL and METRIC methods; this is because the temperature retrieved by both methods is higher when compared to SAFER (Figure S5). This same result is observed by Silva et al. (2019), where they compared METRIC with SAFER obtaining the same result and asserted that the ET_a maximum value, sum and interval by METRIC were higher than in SAFER because the

surface temperature retrieved by SAFER was always higher than that of METRIC, generating lower ET_a values.

The best results across the models evaluated were found in 2018: the SEBAL vs METRIC comparison presented mean values of 0.14, 0.14 and 0.15 mm d^{-1} in 2018 for RMSE, MBE and MAE; however, mean values of 1.61, -1.60 and 1.60 mm d^{-1} were observed in 2020, respectively (Figures 1 and 3). The study by Singh and Senay (2016) found values of 0.92, 0.89 and 0.93 mm d^{-1} for MAE, MBE and RMSE, respectively, for the METRIC model; in addition to reporting that there is some degree of linear relationship between the models tested, emphasizing this tendency for the relationship between METRIC and SEBAL.

SEBAL was developed in the late 1990s, it is considered a worldwide renowned method, and has already been tested in various weather conditions; thus, the comparisons made between METRIC and SAFER found that METRIC presented better data adequacy when compared to the SEBAL standard method. This is due to the methodological structure, as METRIC was designed based on SEBAL's pioneering energy balance process, in which the temperature gradient close to the surface is an indexed function of the radiometric surface temperature, thus eliminating the needs for an absolutely precise surface temperature and for measuring air temperature. Both consider that the latent heat flux varies linearly between the hot and cold pixels, which is based on the logic of the temperature difference between the soil surface and the air (Senay et al., 2007).

Materials and Methods

Study area

The study was conducted in a commercial farm located in the municipality of São Desidério, western region of the state of Bahia, using data from 12 centre pivots (totalling $1,524 \text{ ha}^{-1}$) located in a rectangle and delimited by the $12^{\circ}54'9.80''\text{W}/45^{\circ}29'56.75''\text{S}$ coordinate pair, with a mean altitude of 741 m (Figure 4). According to Köppen's classification, the region's climate is of the Aw type, tropical with rainy summers and dry winters, with annual rainfall varying from 1,000 to 1,300 mm and concentrated between October and April (Alvares et al., 2013).

Meteorological, crop and irrigation management data

Surface meteorological data are important to assist in calibration of the models and in ET_e calculation, estimated through satellite images from the ETM+ and OLI sensors. In this way, data regarding air temperature (T_m , $^{\circ}\text{C}$), wind speed at a height of 2 m (WS, m s^{-1}), solar radiation (R_a , $\text{MJ m}^{-2} \text{ day}^{-1}$), relative humidity (RH, %) and rainfall (R, mm) were used, obtained by means of an automatic weather station, located close to the centre pivots (Figure 4). It was then possible to calculate reference evapotranspiration (ET_0) through the Penman-Monteith method (PM-FAO 56) (Allen et al., 1998). The centre pivots studied are cultivated with cotton, with acquisition of data referring to sowing date (SD), harvest date (HD), cycle length in days (Cycle) and cotton variety used (Va) (Table 1).

Orbital images

Data obtained by satellites Landsat 7 (Enhanced Thematic Mapper Plus [ETM+] spectral sensor, for multispectral bands with 30 m spatial resolution) and Landsat 8 (Operational Land Imager [OLI] and Thermal Infrared Sensor [TIRS] spectral sensors, with spatial resolution for the thermal

bands at 30 and 100 m, respectively) were used, with the scene located in orbit 220, point 69, between 2018 and 2020. Time resolution is 16 days and the images are available free of charge (Pardo-Pascual et al., 2018). The images with no clouds over the study area obtained for each agricultural year are presented in Figure 5.

Methods to estimate effective evapotranspiration (ET_e)

Three models belonging to the SSM class were used to estimate ET_e , namely: SEBAL, METRIC and SAFER. In the selection of the three models for the study, SEBAL was determined as a reference; currently considered as one of the most reliable algorithms for estimating ET, it is one of the most promising approaches for local and regional estimation with minimal soil data (Liou and Kar, 2014), is widely accepted and validated to obtain evapotranspiration (ET) data in agricultural areas (Bastiaanssen et al., 1998), and has already been tested in more than 30 countries around the world with precision varying from 85% to 95% on daily and seasonal scales (Bastiaanssen, 2000; Bastiaanssen et al., 2005).

Standard model - Surface Energy Balance Algorithm for Land (SEBAL)

SEBAL is an image processing model to estimate evapotranspiration (ET) as a residual of the surface energy balance. This model was developed in the Netherlands by Bastiaanssen et al. (1998), with the proposal of estimating the spatial variation of most of the empirically essential hydrometeorological parameters. Requiring only field information on short-wave atmospheric transmittance, surface temperature and vegetation height, in addition to not involving numerical simulation models, it calculates the fluxes regardless of the land cover and it can ultimately deal with thermal infrared images in resolutions from a few meters to a few kilometres (Bastiaanssen, 1998). SEBAL uses surface temperature (T_0), hemispheric surface reflectance (r_0) and the Normalized Difference Vegetation Index (NDVI), as well as their interrelationships, to infer surface fluxes for a wide spectrum of soil types. A simplified form of the SEBAL algorithm can be seen in Equations 1, 2 and 3.

$$\lambda ET = (R_n - G - H) \quad (1)$$

$$ET_{inst} = 3,600 / (\lambda ET - \lambda) \quad (2)$$

$$ET_{24} = ET_r F \times ET_{r,24} \quad (3)$$

Where λET : latent heat flux (W/m^2); R_n : net radiation resulting from the sum of all incoming and outgoing short-wave and long-wave radiation on the surface; G : sensitive heat flux conducted to the soil; H : sensitive heat flux conducted to the air; ET_{inst} : instantaneous ET ($mm\ h^{-1}$); 3,600: second-to-hour conversion; ET_{24} : 24-hour evapotranspiration; $ET_r F$: reference ET fraction; and $ET_{r,24}$: daily ET_r .

In their structure, the SEBAL and METRIC models use the surface temperature (dT) that is indexed to the radiometric surface temperature (Allen et al., 2007). Therefore, T_s uses a simple linear relationship: $dT = a + bT_s$ (where a and b are correlation coefficients of manually-selected hot and cold pixels in the image) (Bhattarai et al., 2016). A hot pixel is selected from a dry and empty agricultural field, where ET is assumed to be 0 while a cold pixel is selected from a well-irrigated crop surface with full coverage, where ET is assumed to be close to a maximum rate (Bastiaanssen et al., 2005). One of the advantages of this model is that it requires few soil-based meteorological data, which makes it useful

for places where these data would be limited (Mkhwanazi et al., 2015).

Mapping Evapotranspiration at High Resolution and with Internalized Calibration (METRIC) model

METRIC is based on the SEBAL model, using the same dT estimation technique, thus eliminating the needs for an absolutely precise aerodynamic surface temperature and for air temperature measurements to estimate sensitive heat flux on the surface (Allen et al., 2007). In addition to that, the energy balance based within a scene is calibrated under two extreme conditions (dry and wet) using locally available meteorological data (Liou and Kar, 2014). For these extreme conditions, ET in the cold (wet) pixel is considered 5% higher than ET_r . Thus, it allows for some H partition for a cold pixel ($H_{cold} = R_n - G - 1.05\lambda ET_r$ and $dT \neq 0$) (Bhattarai et al., 2016). A simplified demonstration of METRIC can be seen in Equations 4, 5 and 6, in which the same concept applied by the SEBAL model occurs in its processes; however, the positive point of this model is that it provides relatively more precise ET estimates in images with higher resolutions when compared to more general models, in addition to considering the impacts of regional advection.

$$ET_{inst} = 3,600(LE/\lambda\rho_w) \quad (4)$$

$$\lambda = [2.501 - 0.00236(T_s - 273.15)] \times 10^6 \quad (5)$$

$$ET_r F = ET_{inst}/ET_r \quad (6)$$

Where ET_{inst} : instantaneous ET ($mm\ h^{-1}$), LE : latent heat flux ($W\ m^{-2}$); ρ_w : water density ($\sim 1,000\ kg\ m^{-3}$); λ : vaporization latent (Jkg^{-1}) representing the heat absorbed when one kilogram of water evaporates and is calculated; $ET_r F$, fraction of the reference ET (ET_r), it is for the 0.5 m height standardized alfalfa reference at the time of the image; T_s : surface temperature (K).

This model was implemented in Google's Earth Engine Evapotranspiration Flux (EEFlux) platform. The EEFlux project was funded by Google Inc., and was supported by three institutions: University of Idaho (UI), University of Nebraska-Lincoln (UNL) and Desert Research Institute (DRI), as well as by the USGS through the Landsat Science Team, where each student and employee had complementary capacity and carried out work components in coordination with the other universities. EEFlux is currently available free of charge at <https://eeflux-level1.appspot.com/>, with a vast collection of processed images from Landsat dating back from 1984 and with updates every 16 days for the same point. In this context, to evaluate the METRIC model estimation, the already processed images from EEFlux were used, corresponding to the same periods for the other methods studied.

Simple Algorithm for Evapotranspiration Retrieving (SAFER) model

The SAFER model was proposed by Teixeira and Hernandez (2012), where they evaluated two models based on the Penman-Monteith (PM) method. Modelling involved net radiation and the soil heat fluxes, the resistance values to the water fluxes and interpolated meteorological data. When used with satellites and a network of agrometeorological stations, both of the simple observation models are suitable for river basin scale implementation for ET monitoring. The equation to calculate ET_e is shown in a simplified form by means of Equation 7.

$$ET_e = \exp \left[a_{sf} + b_{sf} \left(\frac{T_0}{\alpha_0 NDVI} \right) \right] \quad (7)$$

Where \exp : vaporization latent (Jkg^{-1}) representing the heat absorbed when one kilogram of water evaporates and is

calculated as in the equation; a and b are regression coefficients; where $a_{sf} = 1$ and $b_{sf} = -0.008$; T_0 : surface temperature; α_0 : surface albedo; and NDVI: Normalized Difference Vegetation Index.

The NDVI, α_0 and T_0 images are the only input parameters for modelling the ET/ET_0 ratio values using SAFER. The values for this ratio were then multiplied by the daily ET_0 grids to estimate the ET values on this large-scale time scale. New studies such as Teixeira et al. (2017) and Teixeira (2012) were developed for the adaptation of new sensors and indices applied to this model; therefore, they must be consulted to better understand this model. A number of studies developed by Venancio et al. (2020) calibrated the model for the corn crop in western Bahia, finding a and b coefficients of 0.32 and -0.0013, respectively.

Statistical indicators

To evaluate the ET_e estimations, the Root Mean Square Error (RMSE), Mean Bias Error (MBE), Mean Absolute Error (MAE) and coefficient of determination (r^2) indicators were used,

$$RMSE = \sqrt{\frac{\sum_{i=1}^n (ET_{METRIC \text{ and } SAFER} - ET_{SEBAL})^2}{n}} \quad (8)$$

$$MBE = \frac{\sum_{i=1}^n (ET_{METRIC \text{ and } SAFER} - ET_{SEBAL})}{n} \quad (9)$$

$$MAE = \frac{\sum_{i=1}^n (|ET_{METRIC \text{ and } SAFER} - ET_{SEBAL}|)}{n} \quad (10)$$

$$r^2 = \left(\frac{\sum_{i=1}^n (|ET_{SEBAL} - ET_{METRIC \text{ and } SAFER}|)(ET_{METRIC \text{ and } SAFER} - ET_{METRIC \text{ and } SAFER})}{\sqrt{\sum_{i=1}^n (ET_{SEBAL} - ET_{SEBAL})^2 \sum_{i=1}^n (ET_{METRIC \text{ and } SAFER} - ET_{METRIC \text{ and } SAFER})^2}} \right)^2 \quad (11)$$

calculated according to Equations 8 to 11.

These indices were widely used to validate estimation methods such as Costa et al. (2020) and Venancio et al. (2020). The Quantum GIS software was used for image processing. The statistical analyses were performed in the *Estatística* software (StatSoft, Palo Alto, California, USA).

Conclusion

The ET_c data estimated through the METRIC and SAFER models are similar to SEBAL and can be reliably applied in water resource management and, mainly, when seeking estimation methods that consider spatial and time variability, as they contribute to improved decision-making in irrigation management. The comparisons carried out between all three agricultural years presented better performance with the SEBAL vs SAFER models, with mean values of 0.54, -0.30 and 0.31 mm d^{-1} in RMSE, MBE and MAE, respectively. The current study noticed that the data obtained by all three models can be applied to estimate ET_e in irrigated cotton plantations and, consequently, its results can assist in irrigation management and in crop treatments. It is noted that SEBAL is considered a standard model and the study-of-the-art on this method portrays its reliability and precision in several papers applied in all continents. The METRIC model presents an advantage, as a time series of images already processed from the Landsat satellites is available for the ETM+ and OLI sensors, which facilitates acquisition of reliable data to carry out irrigation management. The data can be accessed through the EEFlux platform.

Acknowledgments

To *Universidade Estadual do Oeste do Paraná* (UNIOESTE), *Universidade Tecnológica Federal do Paraná* (UTFPR) and *Coordenação de Aperfeiçoamento de Pessoal de Nível*

Superior (CAPES) - Brazil (Funding Code 001) for funding this project.

References

- Acker J, Williams R, Chiu L, et al (2014) Remote Sensing from Satellites☆. In: Reference Module in Earth Systems and Environmental Sciences. Elsevier, pp 161–202
- Allen DE, Singh BP, Dalal RC (2011) Soil Health Indicators Under Climate Change: A Review of Current Knowledge. In: Singh BP, Cowie AL, Chan KY (eds) Soil Health and Climate Change, 29th edn. Springer, Verlag Berlin Heidelberg, pp 25–45
- Allen R, Pereira LS, Raes D, Smith M (1998) FAO Irrigation and drainage paper 56. Irrig Drain 300:300
- Allen R, Tasumi M, Morse A, et al (2007) Satellite-Based Energy Balance for Mapping Evapotranspiration with Internalized Calibration (METRIC)—Model. J Irrig Drain Eng 133:395–406.
- Alvares CA, Stape JL, Sentelhas PC, et al (2013) Köppen's climate classification map for Brazil. Meteorol Zeitschrift 22:711–728.
- Barker JB, Neale CMU, Heeren DM, Suyker AE (2018) Evaluation of a hybrid reflectance-based crop coefficient and energy balance evapotranspiration model for irrigation management. Trans ASABE 61:533–548.
- Bastiaanssen WGM (2000) SEBAL-based sensible and latent heat fluxes in the irrigated Gediz Basin, Turkey. J Hydrol 229:87–100.
- Bastiaanssen WGM (1998) Remote Sensing in Water Resources Management: The State of the Art, 1st edn. International Water Management Institute, Colombo.
- Bastiaanssen WGM, Molden DJ, Makin IW (2000) Remote sensing for irrigated agriculture: Examples from research and possible applications. Agric Water Manag 46:137–155.
- Bastiaanssen WGM, Noordman EJM, Pelgrum H, et al (2005) SEBAL Model with Remotely Sensed Data to Improve Water-Resources Management under Actual Field Conditions. J Irrig Drain Eng 131:85–93.
- Bastiaanssen WGM, Pelgrum H, Wang J, et al (1998) A remote sensing surface energy balance algorithm for land (SEBAL): 1. Formulation. J Hydrol 212–213:213–229.
- Bhattarai N, Shaw SB, Quackenbush L, et al (2016) Evaluating five remote sensing based single-source surface energy balance models for estimating daily evapotranspiration in a humid subtropical climate. Int J Appl Earth Obs Geoinf 49:75–86.
- Colaizzi PD, Agam N, Tolk JA, et al (2014) Two-source energy balance model to calculate E, T, and ET: Comparison of Priestley-Taylor and Penman-Monteith formulations and two time scaling methods. Trans ASABE 57:479–498.
- Colaizzi PD, Agam N, Tolk JA, et al (2002) Advances in a two-source energy balance model: partitioning of evaporation and transpiration for cotton. Trans ASABE 7004:1–29
- Costa J de O, José JV, Wolff W, et al (2020) Spatial variability quantification of maize water consumption based on Google EEflux tool. Agric Water Manag 232.
- Teixeira AHC, Hernandez FBT (2012) Up scaling guava water balance in the Petrolina/Juazeiro growing area, northeast Brazil. Acta Hort 959:193–200.
- FAO F and A organization of the UN (2021) AQUASTAT - FAO's Global Information System on Water and Agriculture. In: 2021. <https://www.fao.org/aquastat/en/overview/methodology/water-use>. Accessed 3 Apr 2022

- Filgueiras R, Mantovani EC, Althoff D, et al (2019) Dynamics of actual crop evapotranspiration based in the comparative analysis of sebal and metric-eeflux. *Irriga* 1:72–80.
- Jensen JR (2000) *Remote Sensing of the Environment An Earth Resource Perspective*. University of South Carolina, New Jersey
- Jensen ME, Allen R (2016) Evaporation, evapotranspiration, and irrigation water requirements
- Kustas WP, Norman JM (1996) Utilisation de la télédétection pour le suivi de l'évapotranspiration sur les terres. *Hydrol Sci J* 41:495–516.
- Liou YA, Kar SK (2014) Evapotranspiration estimation with remote sensing and various surface energy balance algorithms-a review. *Energies* 7:2821–2849.
- Mkhwanazi M, Chávez JL, Andales AA (2015) SEBAL-A: A remote sensing ET algorithm that accounts for advection with limited data. Part I: Development and validation. *Remote Sens* 7:15046–15067.
- Norman JM, Kustas WP, Humes KS (1995) Source approach for estimating soil and vegetation energy fluxes in observations of directional radiometric surface temperature. *Agric For Meteorol* 77:263–293.
- Pardo-Pascual JE, Sánchez-García E, Almonacid-Caballer J, et al (2018) Assessing the accuracy of automatically extracted shorelines on microtidal beaches from landsat 7, landsat 8 and sentinel-2 imagery. *Remote Sens* 10:1–20. <https://doi.org/10.3390/rs10020326>
- Pianalto FS, Yool SR (2017) Sonoran Desert rodent abundance response to surface temperature derived from remote sensing. *J Arid Environ* 141:76–85.
- Pradipta A, Souplos P, Kourgialas N, et al (2022) Remote Sensing, Geophysics, and Modeling to Support Precision Agriculture—Part 2: Irrigation Management. *Water* 14:1157.
- Sánchez-Aparicio M, Andrés-Anaya P, Del Pozo S, Lagüela S (2020) Retrieving land surface temperature from satellite imagery with a novel combined strategy. *Remote Sens* 12.
- Senay GB, Budde M, Verdin JP, Melesse AM (2007) A coupled remote sensing and simplified surface energy balance approach to estimate actual evapotranspiration from irrigated fields. *Sensors* 7:979–1000.
- Silva CDOF, Manzione RL, Albuquerque Filho JL (2019) Comparison of safer and metric-based actual evapotranspiration models in a subtropical area of Brazil. *IRRIGA* 1:48–55.
- Singh RK, Senay GB (2016) Comparison of four different energy balance models for estimating EvapoTranspiration in the Midwestern United States. *Water (Switzerland)* 8:1–19.
- Small C (2006) Comparative analysis of urban reflectance and surface temperature. *Remote Sens Environ* 104:168–189.
- Sun H (2016) A two-source model for estimating evaporative fraction (TMEF) coupling Priestley-Taylor formula and two-stage trapezoid. *Remote Sens* 8.
- Teixeira AH de C, Leivas JF, Hernandez FBT, Franco RAM (2017) Large-scale radiation and energy balances with Landsat 8 images and agrometeorological data in the Brazilian semiarid region. *J Appl Remote Sens* 11:016030.
- Teixeira AH de d. C, Hernandez FBT, Lopes HL (2012) Application of Landsat images for quantifying the energy balance under conditions of land use changes in the semi-arid region of Brazil. *Remote Sens Agric Ecosyst Hydrol XIV* 8531:85310P.
- Venancio LP, Mantovani EC, Do Amaral CH, et al (2020) Evapotranspiration mapping of commercial corn fields in brazil using safer algorithm. *Sci Agric* 78:1–12.
- Walne CH, Alsajri FA, Gajanayake B, et al (2020) In Vitro Seed Germination Response of Corn, Cotton, and Soybean to Temperature. *J Mississippi Acad Sci* 65:463–469
- Wang XG, Kang Q, Chen XH, et al (2020) Wind Speed-Independent Two-Source Energy Balance Model Based on a Theoretical Trapezoidal Relationship between Land Surface Temperature and Fractional Vegetation Cover for Evapotranspiration Estimation. *Adv Meteorol* 2020:
- Yang L, Li J, Sun Z, et al (2022) Daily actual evapotranspiration estimation of different land use types based on SEBAL model in the agro-pastoral ecotone of northwest China. *PLoS One* 17: